

Array lead zirconate titanate/glass piezoelectric microcantilevers for real-time detection of *Bacillus anthracis* with 10 spores/ml sensitivity and 1/1000 selectivity in bacterial mixtures

John-Paul McGovern, Wei-Heng Shih, Richard F. Rest, Mitali Purohit, Mark Mattiucci et al.

Citation: *Rev. Sci. Instrum.* **80**, 125104 (2009); doi: 10.1063/1.3264082

View online: <http://dx.doi.org/10.1063/1.3264082>

View Table of Contents: <http://rsi.aip.org/resource/1/RSINAK/v80/i12>

Published by the [American Institute of Physics](http://www.aip.org).

Related Articles

Vertical microbubble column—A photonic lab-on-chip for cultivation and online analysis of yeast cell cultures
Biomicrofluidics **6**, 034106 (2012)

Translocation of nanoparticles through a polymer brush-modified nanochannel
Biomicrofluidics **6**, 034101 (2012)

Microfluidic separation of live and dead yeast cells using reservoir-based dielectrophoresis
Biomicrofluidics **6**, 034102 (2012)

Fabrication of paper-based microfluidic device using printed circuit technology
AIP Advances **2**, 022171 (2012)

Microfluidic three-dimensional hydrodynamic flow focusing for the rapid protein concentration analysis
Biomicrofluidics **6**, 024132 (2012)

Additional information on *Rev. Sci. Instrum.*

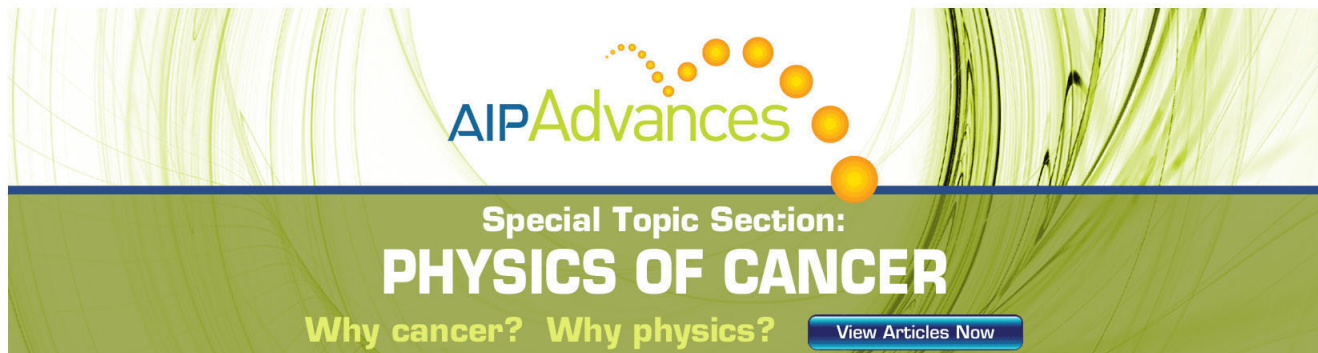
Journal Homepage: <http://rsi.aip.org>

Journal Information: http://rsi.aip.org/about/about_the_journal

Top downloads: http://rsi.aip.org/features/most_downloaded

Information for Authors: <http://rsi.aip.org/authors>

ADVERTISEMENT



AIP Advances

Special Topic Section:
PHYSICS OF CANCER

Why cancer? Why physics? [View Articles Now](#)

Array lead zirconate titanate/glass piezoelectric microcantilevers for real-time detection of *Bacillus anthracis* with 10 spores/ml sensitivity and 1/1000 selectivity in bacterial mixtures

John-Paul McGovern,¹ Wei-Heng Shih,¹ Richard F. Rest,² Mitali Purohit,² Mark Mattiucci,³ Kambiz Pourrezaei,³ Banu Onaral,³ and Wan Y. Shih^{3,a)}

¹Department of Materials Science and Engineering, Drexel University, Philadelphia, Pennsylvania 19104, USA

²Department of Microbiology and Immunology, Drexel University, Philadelphia, Pennsylvania 19104, USA

³School of Biomedical Engineering, Science and Health Systems, Drexel University, Philadelphia, Pennsylvania 19104, USA

(Received 6 July 2009; accepted 26 October 2009; published online 7 December 2009)

An array of three identical piezoelectric microcantilever sensors (PEMSs) consisting of a lead zirconate titanate layer bonded to a glass layer was fabricated and examined for simultaneous, *in situ*, real-time, all-electrical detection of *Bacillus anthracis* (BA) spores in an aqueous suspension using the first longitudinal extension mode of resonance. With anti-BA antibody immobilized on the sensor surfaces all three PEMS exhibited identical BA detection resonance frequency shifts at all tested concentrations, $10\text{--}10^7$ spores/ml with a standard deviation of less than 10%. The detection concentration limit of 10 spores/ml was about two orders of magnitude lower than would be permitted by flexural peaks. In blinded-sample testing, the array PEMS detected BA in three samples containing BA: (1) 3.3×10^3 spores/ml, (2) a mixture of 3.3×10^3 spores/ml and 3.3×10^5 *S. aureus* (SA) and *P. aeruginosa* (PA) per ml, and (3) a mixture of 3.3×10^3 spores/ml with 3.3×10^6 SA+PA/ml. There was no response to a sample containing only 3.3×10^6 SA+PA/ml. These results illustrate the sensitivity, specificity, reusability, and reliability of array PEMS for *in situ*, real-time detection of BA spores. © 2009 American Institute of Physics.

[doi:10.1063/1.3264082]

I. INTRODUCTION

While cell culture¹ and polymerase chain reaction^{2,3} techniques provide specific and sensitive detection of biological agents, they lack real-time assay capability. As such, there is a need for equally reliable, but real-time bioassay detection techniques in applications such as public airspace biodefense monitoring, food and drinking water contamination detection, and military applications.⁴ In these applications, large amounts of time, money, and person power are consumed in consequence management, when confirmation, reaction, and remediation procedures are initiated. Thus, while sensitivity is of utmost importance and presence of biological agents must not be missed, false positives (i.e., false alarm detections) should also be kept to an absolute minimum. To detect miniscule antigen levels while also preventing false positive events, sensitivity and redundancy of biosensor systems are both required. It is desirable to have array sensor systems with high sensitivity to run all redundant assays in parallel. Furthermore, array sensors are also able to run control tests in parallel and in real time. The need for array as opposed to single sensor detection has been identified and attempts at implementation have been made in optical immunofluorescence,^{5–7} fiber-optic,⁸ electrochemical,⁹ nanowire,¹⁰ surface plasmon resonance¹¹ (SPR),

quartz crystal microbalance¹² (QCM), and cantilever^{13,14} systems. Though highly sensitive, optical “on-slide” systems are generally used for protein and DNA detection and require microscopic or optical system interpretation of results and thus are not real time. While some optical methods can be rapid and can test for multiple antigens at once, portability and long-term monitoring are difficult.¹⁵ Some systems developed for such applications demonstrated only modest levels of sensitivity (3×10^5 spores/ml).¹⁶ While portable fiber-optic,¹⁷ SPR,¹¹ and QCM¹⁸ array systems are more easily monitorable, they do not have better sensitivity than traditional optical systems.

Piezoelectric microcantilever sensors (PEMS) consisting of a highly piezoelectric layer bonded to a nonpiezoelectric layer are a new type of biosensors whose *flexural* mechanical resonance that can both be excited and detected by electrical means was used for detection. With receptors immobilized on the PEMS surface, binding of antigens shifts PEMS flexural resonance frequency. Real-time, label-free antigen detection is achieved by electrically monitoring the PEMS flexural resonance frequency shift.^{19–26} PEMS flexural-mode detection sensitivity is related to the thickness and the size of the PEMS. Generally, a PEMS flexural-mode detection sensitivity increases with a reduced PEMS size and thickness.¹⁹ A lead zirconate titanate (PZT)/glass PEMS about 1 mm long consisting of a 127- μm thick commercial PZT layer on a 75–150 μm glass layer with a 2 mm long glass tip generally

^{a)}Electronic mail: shihwy@drexel.edu.

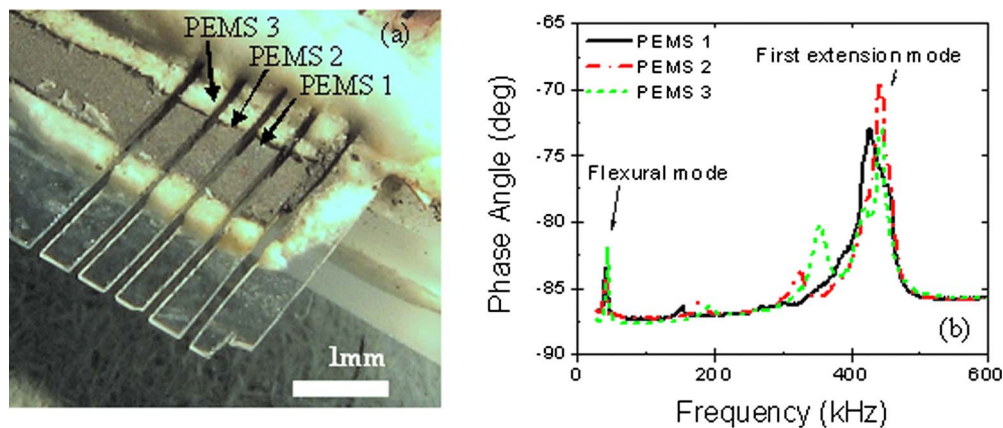


FIG. 1. (Color online) (a) An optical micrograph of array PEMS and (b) resonance spectra with detection peaks indicated.

exhibited a mass detection sensitivity of the order of 10^{-10} g/Hz,^{20–24} while a lead magnesium niobate-lead titanate, $(\text{PbMg}_{1/3}\text{Nb}_{2/3}\text{O}_3)_{0.63}-(\text{PbTiO}_3)_{0.37}$ (PMN-PT)/tin PEMS 600–1200- μm -long consisting of an 8- μm -thick PMN-PT layer bonded with a 5- μm -thick tin layer exhibited a mass detection sensitivity of the order of 10^{-12} – 10^{-13} g/Hz^{23–26} and a PZT/SiO₂ 60- μm -long consisting of a 1- μm -thick PZT thin film on 1- μm -thick SiO₂ layer with a 20-mm-long SiO₂ tip exhibited a mass sensitivity of 10^{-16} g/Hz.²⁷ Due to thickness and size differences, for micrometer-size bacteria detection, a 127- μm -thick PZT/glass PEMS exhibited a concentration limit of 500–1000 bacteria/ml^{20,21} while an 8- μm -thick PMN-PT PEMS exhibited a much lower 36 total spore sensitivity.²⁶

More recent studies showed that PEMS flexural-mode detection resonance frequency shift was primarily due to the elastic modulus change in the piezoelectric layer from the stress induced by the binding of the target analyte to the PEMS surface.^{28,29} As a result, the detection sensitivity of a PMN-PT PEMS and that of a PZT PEMS was, respectively, 300 times^{28,29} and 100 times^{20,21} higher than could be accounted for by mass loading alone. These studies also showed that PEMS could exhibit high-frequency nonflexural resonance modes such as width and length extension modes^{28,30} due to the presence of the highly piezoelectric layer, which silicon-based microcantilevers lack. As nonflexural extension mode resonance occurs at a much higher frequency than flexural-mode resonance, detection using nonflexural resonance modes can potentially increase PEMS sensitivity without size reduction.

The goal of this study is to examine array millimeter-long PZT/glass PEMS for *Bacillus anthracis* (BA) spore detection using the first longitudinal extension mode. We will show that using array millimeter-long PZT/glass PEMS with the first longitudinal mode at around 400 kHz, we were able to detect BA with 10 spores/ml concentration sensitivity and 1/1000 selectivity with respect to *Staphylococcus aureus* (SA) and *Pseudomonas aeruginosa* (PA).

II. EXPERIMENTAL

A. Sensor array

PZT/glass PEMS arrays were fabricated by bonding a 75- μm -thick glass layer to a 127- μm -thick square of PZT

(Piezo Systems, Inc., Cambridge, MA) followed by bonding the PZT/glass assembly onto a substrate of glass microscope slide (Fisher, Fair Lawn, NJ). The glass layer protruded over the edge of the microscope slide by about 3.5 mm and the PZT extended about 1.7 mm over the edge of the slide, i.e., 1.7 mm back from the front edge of the glass layer. This layered structure was then cut with a wire-saw (WS-22, Princeton Scientific, Princeton, NJ) at spacings of 400 μm to achieve the structure shown in Fig. 1(a). Wires were then bonded to the PZT electrodes.

A switch box (3499A, Agilent) and an impedance analyzer (4294A, Agilent), both computer controlled, were used for multiplexed, real-time detection of BA spores in suspension. However, due to limitations of the switch box, as well as cycle-time constraints, only three of the sensors shown in Fig. 1(a) were monitored during detection experiments. The spectra of these sensors are shown in Fig. 1(b). For all three PEMS, the peaks below 100 kHz were flexural peaks. The peaks occurring near 410 kHz (indicated by arrows) were the first extension peaks whose frequency could be predicted by $f=c/4L$ where $L=1.7$ mm was the length and $c=(E_{11}/\rho)^{1/2}$ the sound velocity of the protruding PZT layer with $\rho=7800$ kg/m³ and $E_{11}=62$ GPa being the density and the elastic modulus perpendicular to the poling direction of the PZT layer, respectively.³¹ The numerical factor 4 in the denominator took into account that the PZT layer had a fixed end, and thus the first extension peak occurred when the PZT length equaled a quarter wavelength of the sound.³¹ The first extension peaks at around 410 kHz were the peaks monitored for detection.

For a cantilever with a thickness t , length L , and a sound velocity c , the resonance frequency of a flexural mode is proportional to ct/L^2 whereas that of a longitudinal mode is proportional to c/L . The resonance frequency of a longitudinal mode could be higher than that of a flexural mode by a factor of the order of the aspect ratio, L/t . As can be seen from Fig. 1(b), an extensional mode (longitudinal or width) indeed exhibited a much higher resonance frequency than a flexural mode. There are several advantages of using a higher-frequency extension mode than a flexural mode. The relative resonance frequency shift, $\Delta f/f$, due to detection is only related to $s/E_{ave}t$ where Δf and f are the resonance frequency shifts due to detection and resonance frequency,

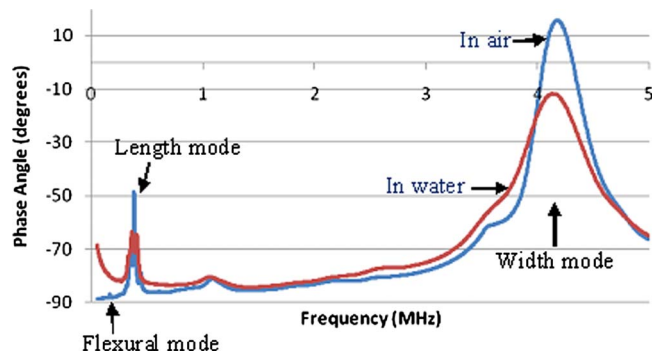


FIG. 2. (Color online) In-air and in-water resonance spectra of MPS-insulated PZT/glass PEMS.

respectively of the PEMS, s , the surface stress due to antigen binding, and t and E_{ave} , the thickness and the average elastic modulus of the PEMS, respectively.²⁹ Therefore, a higher resonance frequency provided by an extension mode can potentially increase the detection resonance frequency shift and enhance the detection sensitivity. In addition, flexural modes are sensitive to liquid damping. A flexural-mode resonance frequency can be greatly reduced and its resonance peak width can be greatly increased in water³² presumably due to its large flexural vibration amplitude. The vibration amplitude of an extension mode is much smaller and can potentially minimize the effect of damping. As an example, we show in Fig. 2 the in-air and in-water resonance spectra of a PZT/glass PEMS electrically insulated by a 3-mercaptopropyltrimethoxysilane (MPS) coating.²³ As can be seen from Fig. 2, the in-water resonance frequency and resonance peak width of the longitudinal mode and those of the width mode remained close to those of the in-air spectrum. Also note that the extensional modes exhibited much higher peak intensity than the flexural modes. The lower-frequency flexural peaks were too low to be seen on the scale in Fig. 2 even in air. Liquid damping further diminished the flexural peaks in water.

B. Bacteria and antibody

BA spores were prepared and inactivated as described in Ref. 22. Likewise, anti-BA spore antiserum was prepared as described in Ref. 22. The anti-BA antibody was immobilized on the MPS insulation coating of PEMS by means of a bifunctional linker, sulfosuccinimidyl-4-(N-maleimido-methyl)cyclohexane-1-carboxylate (sulfo-smcc) as described in Ref. 23.

The anti-BA-spores IgG can cross react with closely related species of BA such as *B. thuringiensis* (BT), *B. cereus* (BC), and *B. subtilis* (BS). However, we have shown that the binding of anti-BA-spore IgG to BT, BC, and BS is much weaker than the binding of anti-BA-spore IgG to BA.²² Binding of close relatives such as BS, BT, BC to anti-BA IgG coated PEMS can be effectively prevented by selecting a flow speed larger than 3.8 mm/s.²² The anti-BA-spore IgG should be selective for BA detection against most other species.

SA and PA are two of the most commonly found bacteria as part of skin flora and most man-made environments

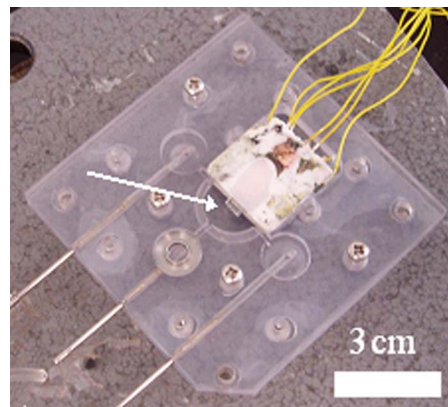


FIG. 3. (Color online) A photograph of the polycarbonate fluidics cartridge with the array PEMS mounted in the center. White arrow indication array PEMS location in the semicircular flow chamber.

throughout the world. They are likely in the background in most of the BA detection. To test the selectivity of BA detection against nonclosely related species, we chose SA and PA as the background for the present study.

SA (ATCC No. 29247) and PA (ATCC No. 35032) were grown on Luria Bertani (LB) agar (Difco-244510, Franklin Lakes, NJ) plates overnight at 37 °C in the presence of 5% CO₂ in air. A colony was then transferred to 10 ml LB broth (Difco-0446-075) in a 50 ml Erlenmeyer flask and grown overnight at 37 °C at 250 rpm. Overnight cultures were diluted and plated to determine concentration. Overnight cultures were washed by centrifugation and suspensions (1×10^9 /ml) in distilled water were inactivated by exposure to ultraviolet (UV) light in a biosafety cabinet in an open plastic Petri dish for 150 min. UV killed bacterial preparations were tested for viability by spreading 100 μ l of inactivated suspension on LB agar plates and checking for colonies the next day. Completely killed bacterial cultures were then resuspended to the appropriate concentration, and mixtures of UV-killed BA, SA, or PA were prepared.

C. Detection procedures

All experiments were performed in a semicircular flow chamber 4.8 mm deep with the flow entering and exiting at its diameter (15 mm). Tubing was connected to this flow chamber and the suspensions were circulated by a Masterflex C/L pump (Model 77120-62, Cole-Parmer, Vernon Hills, IL) at 1 ml/min. The total volume of the fluidics system was 3 ml. The flow system was designed such that the cartridge, together with the PEMS array were a self-contained unit and could be modularly connected to an electrical monitoring and fluidics pumping system in a closed circuit configuration. Several advantages exist for implementing a closed cartridge system such as this. The issue of evaporation of aqueous analyte suspension and resulting requirements of precise dipping depth²¹ and humidity control²⁰ are rendered unnecessary. Once the cartridge system is filled, no analyte liquid is in contact with ambient air and subject to evaporation. This leads to improved sensor stability as well as better temperature stabilization of the PEMS array due to its complete immersion in the aqueous analyte suspension.

TABLE I. Contents of Samples A–D where interferants stand for equal mixtures of SA and PA.

Sample ID	BA spores/ml	Ratio of interferants to BA spores	Interferants/ml
A	3.3×10^3	All BA	0
B	3.3×10^3	100:1	3.3×10^5
C	0	All interferants	3.3×10^6
D	3.3×10^3	1000:1	3.3×10^6

Figure 3 is an image of this cartridge system. The white arrow indicates the location of the PEMS array in the cartridge with the stainless steel pins in the lower left corner of the image allowing for connection to the inlet, outlet and air bleed connections of the fluidics system. During initial filling of the system and subsequent BA detection, the cartridge is oriented with the connection pins upward and the wire leads to the PEMS array downward. Thus, the center connection pin is used as the air-bleed port to ensure that all air bubbles are purged from the system and the left and right connection pins are used as inlet and outlet ports, respectively, for the analyte liquid.

The fluidics system was fabricated entirely out of polycarbonate plastic with silicone rubber used for the gasket layers. This use of polycarbonate and silicone was designed to prevent interactions of the BA spores with surface of the flow chamber, thus enhancing the efficiency of delivery of analyte to the PEMS array biosensor surface. The surface charge of BA spores as well as that of polycarbonate and silicone rubbers is well characterized and all are negative at neutral pH,^{32–34} such as is the case in the de-ionized (DI) water used for experimentation herein. Thus no “sticking” of the BA to the flow system walls was expected and indeed, no adverse effects from such possible sticking was observed.

For a sensitivity study of the PEMS array, two tests were run. First, the array was coated with anti-BA-spore IgG by means of sulfo-SMCC linking molecules (Pierce, Rockford, IL). This sensor was then mounted in the flow chamber and DI water was circulated for 15 min. Following this background period, 10^1 BA spores/ml were added to the system and circulated for a period of 30 min. At 30 min, 90 spores/ml were added to the system, bringing the total number of spores in the system to 100 spores/ml. Again, this concentration was circulated for 30 min. Order of magnitude additions of spores were continued in this manner up to 10^7 spores/ml.

Following this experiment, the sensor array was then cleaned with dilute (1:40 *v:v* in water) piranha solution [1:1 *v:v* 98% sulfuric acid (Fisher, Fair Lawn, NJ):30% hydrogen peroxide (FisherBiotech, Fair Lawn, NJ)], and coated with bovine serum albumin (BSA) on the MPS coating surface using sulfo-smcc as linker in the same fashion as the anti-BA-spore previously. This coating was chosen as a control coating for the PEMS array since BSA is negatively charged,³⁵ as is the *Bacillus* spore coat.³⁶ Thus, nonspecific interaction between the PEMS array and the BA spores was not expected. To verify this hypothesis, the BSA-coated array was subjected to the same BA spore suspensions as was the anti-BA-spore-coated array.

For a study of the selectivity of the PEMS array, a blind study was arranged and administered by one of the co-authors (M.M.). Samples labeled A–D were prepared by the Rest laboratory and provided to the Shih laboratory for experimentation. Experiments were then carried out on the four samples in a similar fashion as in the sensitivity experiments. Namely, the PEMS array was cleaned and immobilized with anti-BA-spore IgG. The array was then mounted in the flow chamber and exposed to DI water for 15 min. Then one of the blind samples was added to the system and circulated for 20 min.

Following the testing of each sample, the PEMS array was cleaned with dilute piranha solution (as above) and re-coated with anti-BA-spore IgG in preparation for the next sample. Unknown until after experimentation, these blinded samples contained mixtures of BA, SA, and PA in DI water at varying concentrations and ratios. Table I details the contents of samples A–D.

III. RESULTS AND DISCUSSIONS

A. Sensitivity

Figure 4(a) shows the resonance frequency shifts versus time of the array PEMS with anti-BA-spore IgG immobilized on the surface when exposed to BA spore suspensions. Squares, circles, and triangles represent the resonance frequency shift of PEMS 1, PEMS 2, and PEMS 3, respectively. Also shown are the resonance frequency shift versus time of the same array PEMS in the same BA suspensions when immobilized with BSA on the surface, rather than anti-BA-spore IgG. The BA spore concentrations during the various 30 min time intervals are indicated by arrows at the point of injection. As can be seen, all three PEMS exhibited no discernable resonance frequency shift when the BSA-coated array PEMS was presented with the full gamut of BA spores.

When the anti-BA-coated array was exposed to 10 BA spores/ml, a frequency shift of approximately 300 Hz was observed on all three PEMS at $t=30$ mins. Then, when the concentration was increased to 100 spores/ml, the frequency shift of the three PEMS decreased another 500 Hz to a total shift of 800 Hz. After each tenfold increase in concentration, the resonant frequencies shifted approximately 500 Hz in the ensuing 30 min up to the concentration increase to 10^6 spores/ml. It can then be seen that saturation of the sensors seemed to occur at approximately 165 min, during the middle of the exposure to 10^6 spores/ml. Finally, no additional frequency decrease was observed upon addition of 10^7 spores/ml, probably due to the saturation of BA binding. For all detections at all concentrations, all three PEMS

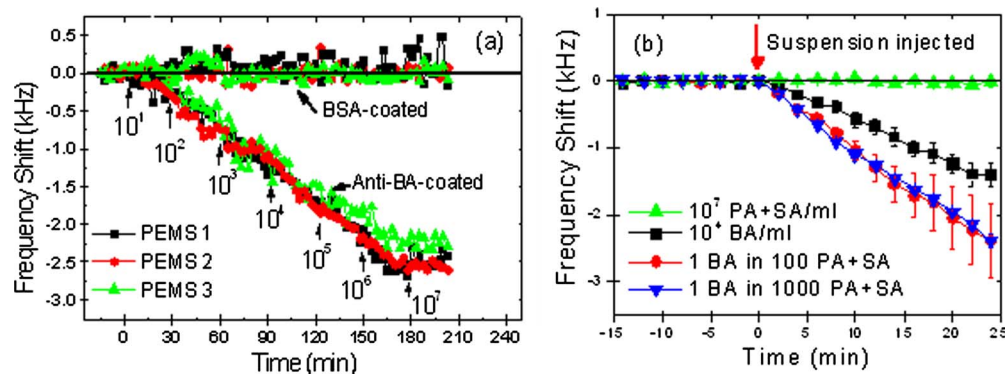


FIG. 4. (Color online) (a) Resonance frequency shift vs time of anti-BA- and BSA-coated PEMS array in BA suspensions of various concentrations, and (b) resonance frequency shift vs time of anti-BA coated PEMS array in BA suspensions in the presence of excess SA and PA cells. Arrows in (a) indicate the times of suspension injection into the flow chamber.

exhibited similar resonance frequency shifts with a standard deviation of about 10% among the three PEMS [Fig. 4(a)]. This clearly illustrates the repeatability and reliability of the PEMS as a sensor for *in situ*, real-time, in-liquid biodection.

During the 15 min leading up to both experiments, the noise levels of the sensor in DI water were 42, 48, and 26 Hz for PEMS 1, PEMS 2, and PEMS 3, respectively. During exposure of the BSA-coated array to the BA spore concentrations, noise levels of 80, 140, and 85 were observed. The anti-BA-spore-coated sensors exhibited noise levels of 60, 75, and 53 Hz during detection of BA spores. Thus, all noise levels were at or below 140 Hz. Even with the worst-case noise level of 140 Hz, the -300 Hz resonance frequency shift for the detection of 10^1 BA spores/ml gives a signal to noise ratio (SNR) of greater than 2. Detections of all other concentrations give an SNR far larger than this, indicating that all observed resonance frequency shifts are true positive responses.

Note that Fig. 4(a) is not a typical dose response plot where the antigen concentration is kept constant. In Fig. 4(a) the concentration of BA was increased by tenfold every 15 min. This is why it looks like the resonance frequency shift kept increasing with time. In response to the concentration increase every 15 min, the resonance frequency shift continued to increase. This does not mean that the final detection needs to take this long. From our earlier studies, a typical saturation time ranges from a few minutes at higher concentrations, e.g., 10^5 spores/ml to 15–30 min at lower concentrations, e.g., 10^1 spores/ml.^{20–23,26} The present detection scheme allowed us to detect BA over a wide range of concentrations, 10^1 – 10^7 spores/ml over a short time. While these experiments did not yield a linear dose response of the PEMS to these concentrations of BA, which would require preparing the sensor surface after detection at each concentration, they nonetheless amply demonstrated the “repeatability” of the detection from sensor to sensor, which is one of the main goals of this study.

B. Selectivity

The sensitivity experiments showed that there was negligible, if any, nonspecific binding of BA spores to the sensor

surface when it was coated with BSA, i.e., there were no “false positive” responses on a BSA-coated array. Selectivity experiments were aimed to further probe this possibility, but also test for a false negative response when other bacterial species (i.e., interferants) were added to the BA spore suspensions.

Figure 4(b) depicts the resonance frequency shift versus time obtained in these blind selectivity experiments. For clarity, the resonance frequency shifts of the three PEMS during exposure to each sample are plotted as average shifts with standard deviations. Sample C produced no resonance frequency shift, sample A produced a resonance frequency shift of 1.3 kHz at 20 min and samples B and D produced resonance frequency shifts of 1.9 and 2.0 kHz at 20 min, respectively. After completion of all testing, these results were compared to the blind sample compositions, shown in Table I. We see that 3.3×10^6 interferants/ml produced no frequency shift in any of the PEMS. The sample containing just 3.3×10^3 BA spores/ml resulted in an average frequency shift of 1.3 kHz for each of PEMS. This shift was consistent with a similar concentration in the sensitivity studies. Finally, samples B and D, both of which contained 3.3×10^3 BA spores but also contained 3.3×10^5 and 3.3×10^6 , respectively, SA and PA cells/ml, produced nearly identical resonant frequency shifts of 2.0 kHz at 20 min. Again, all three PEMS exhibited identical responses in all detections with a standard deviation of about 10% [Fig. 4(b)]. The higher standard deviation of sample B was due to the formation of a bubble toward the later part of the detection.

From these comparisons, it is clear that the array PEMS correctly detected the presence or absence of BA in all four blinded samples. The all-interferant mixture, sample C, produced no false positive response. Furthermore, as evident in the response to samples B and D, the presence of high concentrations of interferants in a suspension of BA did not cause a false negative response, i.e., the interferants did not prevent the positive detection of BA spores.

Interestingly, the interferants seemed to augment the resonance frequency shift in the detection of the BA spores, in that the resonant frequency shifts in the mixtures of BA, SA, and PA (samples B and D) were greater than that in the

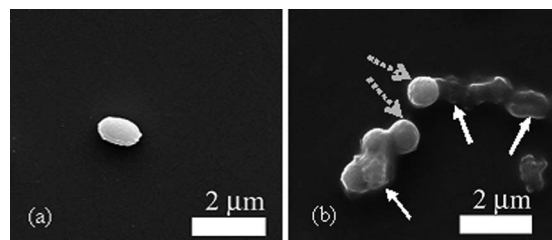


FIG. 5. SEM micrograph of PEMS sensor surface after exposure to (a) sample A -3.3×10^3 BA spores/ml, and (b) sample D -3.3×10^3 BA spores/ml with a 3.3×10^6 cells/ml of SA and PA mixture. The solid arrows in (b) indicate BA spores which are cigar-shaped as shown in (a) while the dashed arrows indicate SA cells which are spherical.

presence of BA alone (sample A). A first reaction to this observation would be to assume that the interferants were nonspecifically sticking to the sensor surface, thus artificially increasing the array response. However, this was clearly not the case as sample C showed that no PEMS array response occurred when a mixture of only interferants was presented. The next conclusion to be drawn is that one or both of the interferants was agglomerating or clumping with the BA spores in suspension. Then, when the BA spore of an agglomerate contacted the anti-BA-spore-coated sensor surface, the whole agglomerate bound to the surface, and thus induced a greater resonant frequency shift than would just a lone spore. This explanation becomes plausible when it is noted that SA possesses a more neutral³⁷ surface charge than that of *Bacillus* spores,³⁶ allowing for such agglomeration.

To further examine the cause of the exaggerated resonance frequency shift in the presence of SA and PA, scanning electron microscopy (SEM) (FEI, XL30) was used to examine the PEMS surfaces after exposure to these samples. As an example, for sample A (3.3×10^3 BA spores/ml) there is a single BA spore bound to the PEMS surface in the area of the electron micrograph [Fig. 5(a)]. This degree of surface coverage is typical of the entire sensor surface. SEM examination showed that no cells adhered to a PEMS sensor surface after exposure to sample C (3.3×10^6 SA+PA cells/ml) (not shown), which is consistent with the negligible resonance frequency shift exhibited by the PEMS in sample C. After exposure to sample D (3.3×10^3 BA spores/ml with 3.3×10^6 SA+PA cells/ml), agglomerates of spores and cells are seen to be bound to the sensor surface [Fig. 5(b)]. In this image, we see several biological entities on the sensor surface in close proximity. The geometries of the three possible cells/spores enable visual differentiation and identification. SA cells are exclusively spherical; PA cells are decidedly elongated with typical aspect ratios (the ratio of length to width) greater than 2. BA spores are slightly elongated with aspect ratios between 1.2 and 1.5. Thus, we can see in Fig. 5(b), no PA is observed on the sensor surface while SA (as indicated by dashed arrows) is observed to be agglomerated with BA (as indicated by solid arrows) on the surface.

With the augmentation of resonance frequency shift of the PEMS array due to BA in the presence of SA, the ability to quantify the exact amount of BA in the analyte solution is affected to a certain degree. However, the main focus of this

study is to demonstrate the ability of the array PEMS to selectively detect BA in the presence of interferants without instance of false positives or false negatives. The issue of reducing or accounting for a possible clumping or agglomeration effect on quantifying the presence of BA will be addressed in a future study.

IV. CONCLUSIONS

This work demonstrated the fabrication, implementation, and initial study of an array system of three identical PZT/glass PEMS for use in biodetection applications. Identical detection of BA spores at a concentration as low as 10 spores/ml was demonstrated using the first longitudinal extension peak and positive detection of BA spores in 1:1000 suspensions of interferant cells was shown by all three PEMS with a standard deviation of less than 10% and without instance of false positive or false negative results. Thus, effective, reliable, all-electrical, real-time, *in situ* array biodetection has been achieved without the need for laser monitoring, advanced optical systems, or laboratory interpretation of results.

ACKNOWLEDGMENTS

This document is disseminated under the partial sponsorship of the United States Department of Transportation, Federal Transit Administration, in the interest of information exchange. The United States Government assumes no liability for the contents or use thereof. The United States Government does not endorse products or manufacturers. Trade or manufacturers' names appear herein solely because they are considered essential to the contents of the report. This work was also supported in part by National Institutes of Health (NIH) Grant No. R01 EB00720 (W.Y.S. and W.H.S.) and Drexel University College of Medicine.

- ¹R. K. Oshiro, Method 1604, US EPA Office of Water (4303T), Washington, D.C., 2002.
- ²I. Sunnotel, C. J. Lowery, J. E. Moore, J. S. G. Dooley, L. Xiao, B. C. Millar, P. J. Rooney, and W. S. Snelling, *Lett. Appl. Microbiol.* **43**, 7 (2006).
- ³L. Xiao, A. Singh, J. Limor, T. K. Graczyk, S. Gradus, and A. Lal, *Appl. Environ. Microbiol.* **67**, 1097 (2001).
- ⁴C. R. Kline, Jr., *IEEE Engineering in Medicine and Biology* **21**, 43 (2002).
- ⁵S. P. Fitzgerald, J. V. Lamont, R. I. McConnell, and E. O. Benchikh, *Clin. Chem.* **51**, 1165 (2005).
- ⁶C. A. Rowe, L. M. Tender, M. J. Feldstein, J. P. Golden, S. B. Scruggs, B. D. MacCraith, J. J. Cras, and F. S. Ligler, *Anal. Chem.* **71**, 3846 (1999).
- ⁷E. D. Lester, G. Bearman, A. Ponce, *IEEE Engineering in Medicine and Biology* **23**, 130 (2004).
- ⁸J. A. Ferguson, F. J. Steemers, and D. R. Walt, *Anal. Chem.* **72**, 5618 (2000).
- ⁹P. Ertl, M. Wagner, E. Corton, and S. R. Mikkelsen, *Biosens. Bioelectron.* **18**, 907 (2003).
- ¹⁰G. Zheng, F. Patolsky, Y. Cui, W. U. Wang, and C. M. Lieber, *Nat. Biotechnol.* **23**, 1294 (2005).
- ¹¹T. M. Chinowsky, S. D. Soelberg, P. Baker, N. R. Swanson, P. Kauffman, A. M. Mactutis, M. S. Grow, R. A. Atmar, S. S. Yee, and C. E. Furlong, *Biosens. Bioelectron.* **22**, 2268 (2007).
- ¹²C. Yao, Q. Chen, M. Chen, B. Zhang, Y. Luo, Q. Huang, J. Huang, and W. Fu, *J. Nanosci. Nanotechnol.* **6**, 3828 (2006).
- ¹³A. P. Davila, J. Jang, A. K. Gupta, T. Walter, A. Aronson, and R. Bashir, *Biosens. Bioelectron.* **22**, 3028 (2007).
- ¹⁴K. Ong, K. Zeng, X. Yang, K. Shankar, C. Ruan, and C. Grimes, *IEEE Sens. J.* **6**, 514 (2006).

- ¹⁵J. Karasinski, S. Andreescu, and O. A. Sadik, *Anal. Chem.* **77**, 7941 (2005).
- ¹⁶B. J. Hindson, M. T. McBride, A. J. Makarewicz, B. D. Henderer, U. S. Setlur, S. M. Smith, D. M. Gutierrez, T. R. Metz, S. L. Nasarabadi, K. S. Venkateswaran, S. W. Farrow, B. W. Colston, Jr., and J. M. Dzenitis, *Anal. Chem.* **77**, 284 (2005).
- ¹⁷C. C. Jung, E. W. Saaski, D. A. McCrae, B. M. Lingerfelt, and G. P. Anderson, *IEEE Sens. J.* **3**, 352 (2003).
- ¹⁸H. Zeng, H. Wang, F. Chen, H. Xin, G. Wang, L. Xiao, K. Song, D. Wu, Q. He, and G. Shen, *Anal. Biochem.* **351**, 69 (2006).
- ¹⁹J. W. Yi, W. Y. Shih, and W. H. Shih, *J. Appl. Phys.* **91**, 1680 (2002).
- ²⁰Q. Zhu, W. Y. Shih, and W.-H. Shih, *Sens. Actuators B* **125**, 379 (2007).
- ²¹Q. Zhu, W. Y. Shih, and W.-H. Shih, *Biosens. Bioelectron.* **22**, 3132 (2007).
- ²²J.-P. McGovern, W. Y. Shih, R. Rest, M. Purohit, and Y. Pandia, *Analyst (Lond.)* **133**, 649 (2008).
- ²³J. Capobianco, W. Y. Shih, and W.-H. Shih, *Rev. Sci. Instrum.*, **78**, 046106 (2007).
- ²⁴J. Capobianco, W. Y. Shih, W.-H. Shih, Q.-A. Yuan, and G. P. Adams, *Rev. Sci. Instrum.* **79**, 076101 (2008).
- ²⁵J. Capobianco, W. Y. Shih, and W.-H. Shih, *Rev. Sci. Instrum.* **77**, 125105 (2006).
- ²⁶J.-P. McGovern, W. Y. Shih, and W.-H. Shih, *Analyst (Lond.)* **132**, 777 (2007).
- ²⁷Z. Shen, W. Y. Shih, and W.-H. Shih, *Appl. Phys. Lett.* **89**, 023506 (2006).
- ²⁸Q. Zhu, W. Y. Shih, and W.-H. Shih, *Appl. Phys. Lett.* **92**, 183505 (2008).
- ²⁹Q. Zhu, W. Y. Shih, and W.-H. Shih, *J. Appl. Phys.* **104**, 074503 (2008).
- ³⁰Q. Zhu, W. Y. Shih, and W.-H. Shih, *Appl. Phys. Lett.* **92**, 033503 (2008).
- ³¹J. McGovern, Ph.D. thesis, Drexel University, Philadelphia, PA 19104, 2008.
- ³²J. K. Beattie, *Lab Chip* **6**, 1409 (2006).
- ³³M. T. Khorasani, S. MoemenBellah, H. Mirzadeh, and B. Sadatnia, *Colloids Surf. B Biointerfaces* **51**, 112 (2006).
- ³⁴H. Mamane-Gravetz and K. G. Linden, *J. Appl. Microbiol.* **98**, 351 (2005).
- ³⁵N. Watanabe, T. Shirakawa, M. Iwahashi, and T. Seimiya, *Colloid Polym. Sci.* **266**, 254 (1988).
- ³⁶J. Peng, W. C. Tsai, and C. C. Chou, *Int. J. Food Microbiol.* **65**, 105 (2001).
- ³⁷J. S. Dickson and M. Koohmaraie, *Appl. Environ. Microbiol.* **55**, 832 (1989).